Electron. Mater. Lett., Vol. 10, No. 1 (2014), pp. 253-258
DOI: 10.1007/s13391-013-3170-7

Structure and Electrochemical Behavior of $LiMnBO_3$ Synthesized at Various Temperatures

Yong-Suk Lee[1] and Hyukjae Lee[2,*]

[1] Wolfram Korea Co. Yongin, Gyeonggi 449-880, Korea
[2]Materials Research Center for Energy and Green Technology, Andong National University, Andong, Gyeongbuk 760-745, Korea

(received date: 8 June 2013 / accepted date: 25 June 2013 / published date: 10 January 2014)

$LiMnBO_3$ is synthesized via solid state reaction at various calcination temperatures, in order to investigate their lithium electrochemical behavior for Li-ion batteries. At lower calcination temperature, $LiMnBO_3$ is composed of mostly monoclinic phase, with a small amount of hexagonal phase, but the ratio of hexagonal/monoclinic phase increases with an increase of calcination temperature, resulting in almost pure hexagonal phase at 800°C. Generally, monoclinic/hexagonal mixed phased $LiMnBO_3$ displays better lithium electrochemical performance. While the pristine $LiMnBO_3$ shows very low capacity, carbon-incorporated $LiMnBO_3$ shows hugely improved charge-discharge capacity, in all samples. The maximum capacity, 108.2 mAh/g after 50 cycles, is obtained from $LiMnBO_3$/C composite calcined at 600°C.

Keywords: borates, calcination temperatures, Li-ion batteries, cathode materials

1. INTRODUCTION

Since the first commercial Li-ion batteries were introduced in the early 1990s by Sony, Li-ion batteries have been the primary system for secondary batteries, because of their high capacity, excellent cycle capability, and high energy density.[1,2] However, the material system has not changed much from the original Li-ion batteries, so that the primary cathode and anode materials are still layered oxides and carbon, respectively. As the application of the Li-ion battery has expanded, the current material system of the Li-ion battery, especially in cathode material, shows issues of toxicity, safety, and cost, which prevent the utilization of the Li-ion battery from large scale applications, like electric vehicles and electrochemical storage systems. Thus, many efforts have been made to find new cathode materials to meet the demand.[3-8] Among them, $LiFePO_4$ is the most notable example, because it has both excellent thermal stability and fast ion transport via its olivine structure, which is a three-dimensional framework made up of PO_4 tetrahedra and MO_6 octahedra. $LiFePO_4$ as a cathode material in Li-ion battery was first commercialized by A123. Although $LiFePO_4$ is commercialized successfully, its relatively low energy density (~3.3 V cell voltage and ~170 mAh/g capacity) initiated a search for alternative cathode materials with higher energy density, leading to investigations in many polyanion-based cathode materials, including silicates and borates.[9-15]

Theoretically, borate-based material can be a wonderful cathode material, since borate has low molecular weight and high electronegativity, which can lead to high gravimetric capacity and strong inductive effect, for larger cell voltage for borate-based cathode. Experimentally, however, borate-based electrode materials have not shown a strong candidacy for an alternative cathode material. Legagneur *et al.* first explored the Li electrochemical behavior of $LiMBO_3$ (M = Fe, Mn, and Co),[11] but their work showed that only a small amount of Li-ion could be reversibly inserted/deinserted in $LiMBO_3$. Since then, a few investigations have been conducted on $LiFeBO_3$[12,13] and $LiMnBO_3$,[14-16] and the results have shown some improvements from the original work by Legagneur. Yamada *et al.*[12] could achieve a capacity of ~190 mAh/g for $LiFeBO_3$/C, by avoiding surface poisoning from exposure to ambient atmosphere. Kim *et al*. synthesized monoclinic and hexagonal phase $LiMnBO_3$ using a conventional solid state synthesis, and a maximum second discharge capacity of 100 mAh/g was achieved for carbon coated monoclinic $LiMnBO_3$.

Like $LiMPO_4$, $LiMBO_3$ has intrinsically low electronic and ionic conductivity. Thus, the utilization of a conducting agent, such as carbon, and/or the reduction of the particle size, would improve the lithium electrochemical performance, as proven for $LiMPO_4$.[4-8] As a first part of a work for developing a borate-based cathode material, we investigated the solid state synthesis of $LiMnBO_3$ at various temperatures, and their lithium electrochemical behavior with/without carbon-incorporation. The results demonstrated that the carbon-incorporation and monoclinic/hexagonal mixed phase

*Corresponding author: hlee@anu.ac.kr

could greatly improve the electrochemical performance of $LiMnBO_3$.

2. EXPERIMENTAL PROCEDURE

$LiMnBO_3$ powders were prepared, by mixing stoichiometric amounts of Li_2CO_3, $MnCO_3$, and H_3BO_3. The precursors were dispersed into acetone, and then ball milled for 7 h in a planetary mill with a rotating speed of 250 rpm. After evaporating acetone in a vacuum oven at 57°C for 24 h, the resulting powder was calcined at 500°C - 800°C for 10 h, in an Ar-flowing tube furnace. For $LiMnBO_3$/C composite, 10 wt. % of ketjen black was added into the starting powder, and subsequent solid state procedure was carried out. For carbon coating on $LiMnBO_3$, 10 wt. % of sucrose was added into the starting powder.

In order to analyze the crystal structure, x-ray diffraction (XRD) measurement was conducted, using a Rigaku D/MAX 2000, with Cu Kα radiation in the range between 10° to 80°. The obtained XRD pattern was later used for Rietveld refinement, using the GSAS package. The particle size and morphology were investigated using a scanning electron microscope (SEM: JSM-6700F, JEOL), and transmission electron microscope (TEM: JEM-2010, JEOL).

For electrochemical measurement, coin type half cell (CR2032) was constructed in an Ar-filled glove box. The working electrode was composed of 80 wt. % active material, 10 wt. % Super P carbon black, and 10 wt. % KF-1100 binder in an N-methyle-2-pyrrolidone (NMP) solvent. The slurries were coated onto aluminum foil, dried at 60°C, and roll pressed before assembly. 1.3 M $LiPF_6$ in a mixture of ethylene carbonate and dimethyl carbonate (EC/DMC, 3 : 7 in volume), Celgard 2400, and Li metal foil were used as the electrolyte, the separator, and the counter electrode, respectively. The cells were galvanostatically charged and discharged at 1/20C (1C = 222 mA/g), over a voltage range of 2.0 - 4.5 V vs. Li^+/Li, using a battery cycler (WonATech, WBCS3000). Electrochemical impedance spectroscopy was conducted in the frequency range from 10^6 Hz to 1 mHz, with an amplitude of 5 mV (PAR, Versastat3).

3. RESULTS AND DISCUSSION

$LiMnBO_3$ is known to have two crystal structures. The hexagonal structure consists of MnO_5 square pyramids, planar BO_3 groups, and LiO_4 tetrahedra. The MnO_5 pyramids form chains along the *c*-axis, by sharing of equatorial edges with two adjacent pyramids, and the planar BO_3 groups link three chains via corner sharing, parallel to the [001] direction. LiO_4 tetrahedra also form chains parallel to the MnO_5 pyramids along the *c*-axis, with Li atoms in tetrahedral sites.[11] The monoclinic structure has trigonal bipyramidal MnO_5, which forms polyhedral chains by edge sharing along the [–101] direction. Similar to the hexagonal structure, trigonal planar BO_3 groups link three chains via corner sharing, and Li atoms occupy tetrahedral sites.[17]

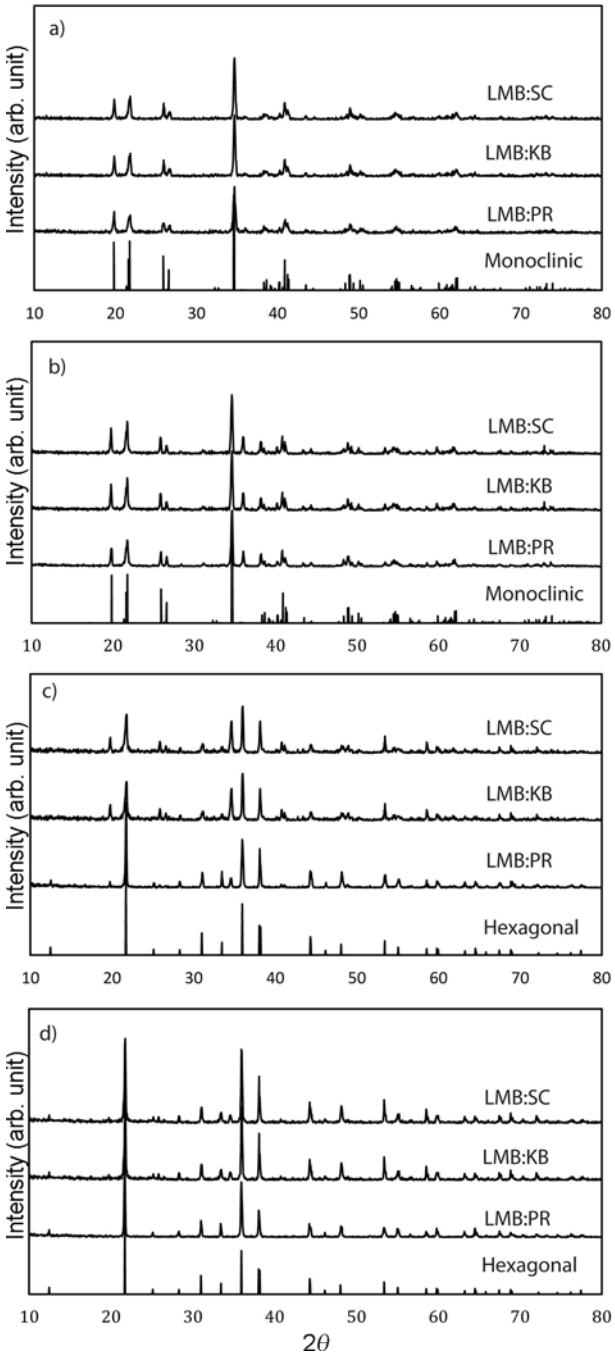

Fig. 1. XRD patterns of $LiMnBO_3$ calcined at (a) 500°C, (b) 600°C, (c) 700°C, and (d) 800°C.

By firing at various temperatures, it was possible to obtain both monoclinic and hexagonal structures. Figure 1 shows XRD patterns of $LiMnBO_3$ synthesized at various temperatures, and with different treatments. Hereafter, for the sake of brevity, the $LiMnBO_3$ powder prepared without any carbon-

incorporation will be denoted as LMB:PR, the $LiMnBO_3$/C composite with ketjen black will be denoted as LMB:KB, and the carbon coated $LiMnBO_3$ using sucrose will be denoted as LMB:SC. When calcined at 500°C, mostly pure monoclinic phase $LiMnBO_3$ was obtained, but the small peak at 35.5° in Fig. 1(a) suggests the presence of a small amount of hexagonal phase. The carbon-incorporated powders (LMB:KB and LMB:SC) do not show noticeable difference from the pristine one. At 600°C calcination temperature, the monoclinic phase is still the dominant phase, but the intensity of the hexagonal peak at 35.5° is relatively high, and other hexagonal peaks, such as at 28° and 31°, are also apparent, suggesting the higher fraction of the hexagonal phase, as the calcination temperature increases. Figure 1(c) shows that the hexagonal phase becomes the dominant phase at the calcination temperature of 700°C, although monoclinic peaks are evident at 19.8° and 34.5°. At 800°C, the dominancy of the hexagonal phase is more pronounced, as most monoclinic peaks disappear in Fig. 1(d). It is interesting that the carbon-incorporated powders show larger monoclinic peaks as compared to pristine powders above 700°C, where the hexagonal phase is dominant, implying that the incorporated carbon might hinder the phase transformation from monoclinic to hexagonal phases. Based on Rietveld refinement analysis, the fractions of monoclinic phase in LMB:PR calcined at 500°C, 600°C, 700°C, and 800°C are determined to be 88%, 66%, 39%, 1.1%, respectively. Figure 2 shows one of the Rietveld refinements on the monoclinic phase (LMB:PR at 500°C).

SEM images of differently prepared $LiMnBO_3$ samples calcined at 500°C and 800°C are shown in Fig. 3. LMB:PR calcined at 500°C (Fig. 3(a)) has agglomerated clusters that consist of small particles and some large particles. The particles in the LMB:PR calcined at 800°C are very large and isolated, as shown in Fig. 3(d). In fact, the particle size increased gradually with increasing calcination temperature (although samples fired at 600°C and 700°C are not shown here), suggesting particle growth during high temperature calcination. The added ketjen black and sucrose seemed to suppress the excessive particle growth during calcination. At the calcination temperature of 500°C, the particle sizes of LMB:KB and LBM:SC are not much different from the size of small particles shown in Fig. 3(a); however, the large particles shown in Fig. 3(a) are not observed in Figs. 3(b) and 3(c). Moreover, LMB:KB and LBM:SC calcined at 800°C show much smaller particles that those in LMB:PR, as shown in Figs. 3(d-f). Since small particles are normally favorable for the lithium electrochemical behavior, the effect of the ketjen black and sucrose could be huge. Figure 4 shows a TEM image of LBM:SC calcined at 500°C, in which the carbon is shown on the surface of particles. The elementary analysis revealed the carbon content of the LMB:SC calcined at various temperature was 3.3 - 3.9 wt. %.

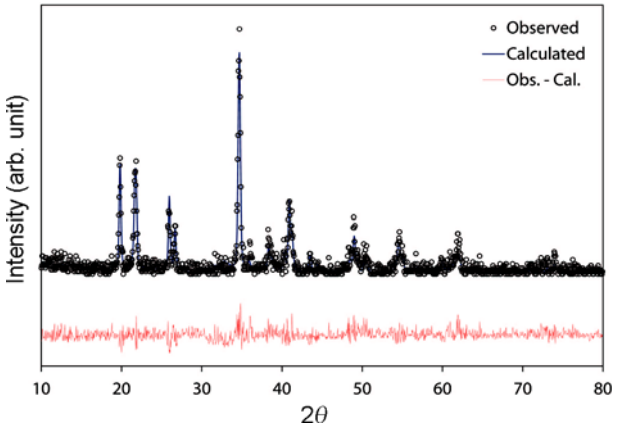

Fig. 2. Plot of Rietveld profile matching of the pristine $LiMnBO_3$ calcined at 500°C.

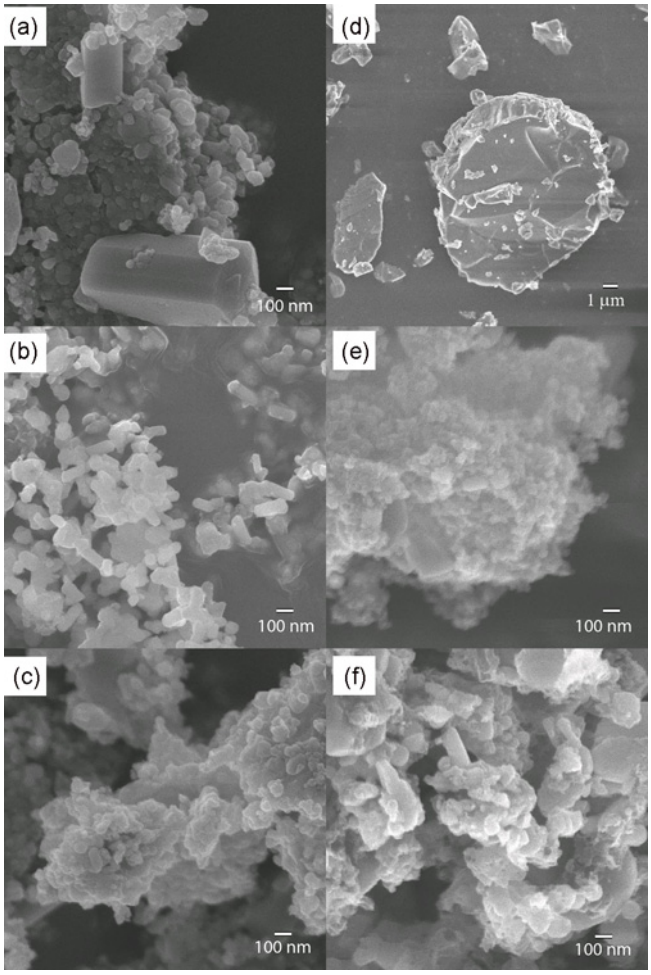

Fig. 3. SEM images of $LiMnBO_3$ calcined at 500°C: (a) LMB:PR, (b) LMB:KB, and (c) LMB:SC, and 800°C: (d) LMB:PR, (e) LMB:KB, and (f) LMB:SC.

Figure 5 displays second charge and discharge profiles of variously prepared $LiMnBO_3$ at a C/20 rate. Overall, the pristine $LiMnBO_3$ shows very limited capacity (less than

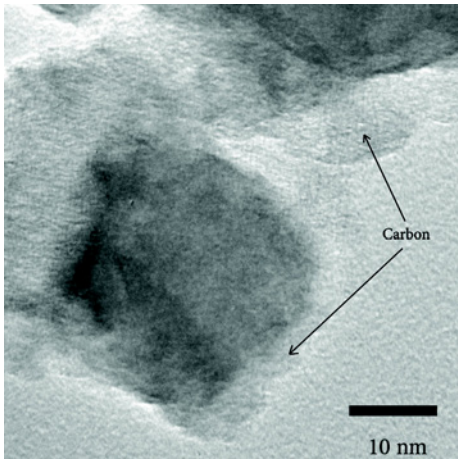

Fig. 4. TEM image of LBM:SC calcined at 500°C.

50 mAh/g), while the monoclinic-rich $LiMnBO_3$ has a little bit higher capacity than that of hexagonal-rich $LiMnBO_3$. $LiMnBO_3$ calcined at 600°C, which consists of 66% monoclinic and 34% hexagonal phase, has the highest capacity. The carbon-incorporation reduced polarization and enhanced capacity significantly at all calcination temperatures, and the higher capacities are found in monoclinic-rich $LiMnBO_3$ in Figure 5. This improved lithium electrochemical behavior can be explained by the increase in conductivity, and the smaller particle sizes (via suppressing excessive particle growth at higher temperatures) by the added carbon. In all figures in Fig. 5, charge and discharge curves are continuously changed with capacity, without any noticeable plateau, indicating that there is no phase transition during lithiation and delithiation. Similar results were obtained in previous studies.[15,16]

The cyclic performance of $LiMnBO_3$ is shown in Fig. 6, in which the charge capacities of differently prepared samples display up to 50 cycles. It is clear that the $LiMnBO_3$ fired at 600°C has the highest capacity in all cases, such that the capacity of LMB:PR, LMB:KB, and LMB:SC samples at the 50th cycle are 16.1, 108.2 and 86.2 mAh/g, respectively. Considering that the monoclinic $LiMnBO_3$ showed higher capacity than the hexagonal counterpart in the previous study, this result is not surprising; however, it is very interesting that the mixed phase $LiMnBO_3$ shows better capacity than that of relatively pure $LiMnBO_3$, although the monoclinic–rich $LiMnBO_3$ (Fig. 6(b)) shows higher capacity than that of the hexagonal-rich $LiMnBO_3$ (Fig. 6(c)). The reason is not clear, but it can be postulated that the presence of hexagonal phase might give an alternative route for Li ion diffusion and, in turn, improve the performance, when the Li ion diffusion path in the monoclinic $LiMnBO_3$ is blocked. It is reported that the monoclinic $LiMnBO_3$ has a one-dimensional Li ion diffusion path, which can be easily blocked by defect.[15] Further study is needed to elucidate the

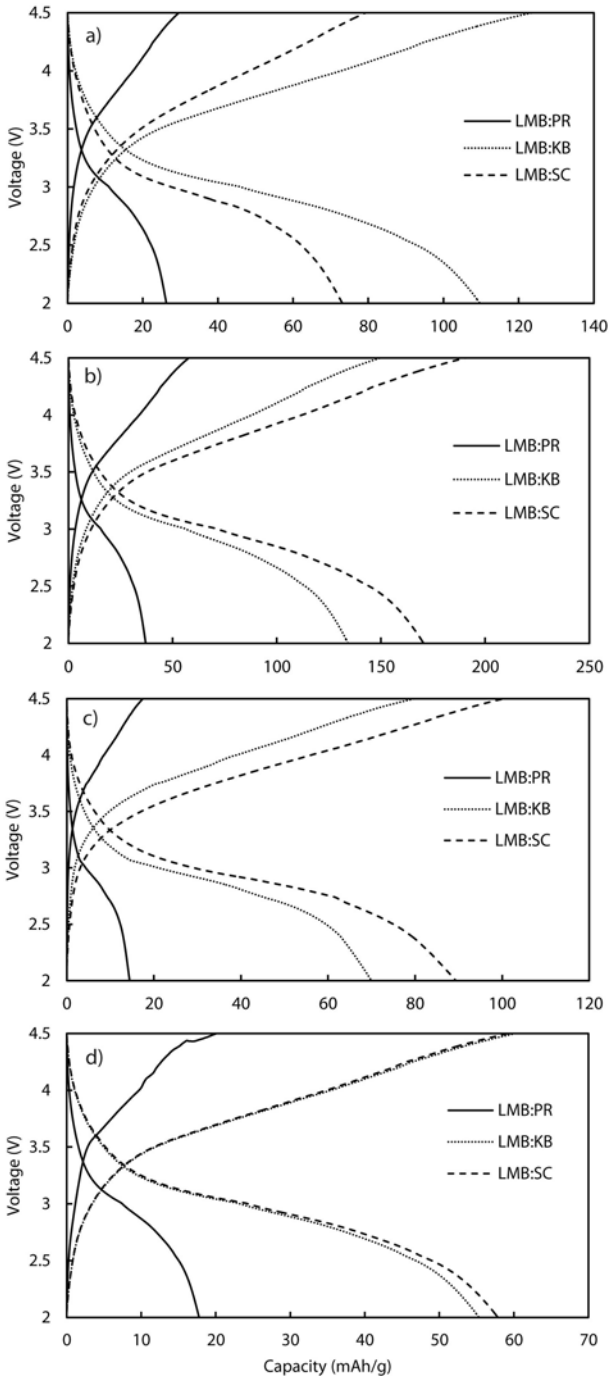

Fig. 5. Voltage profiles of $LiMnBO_3$ calcined at (a) 500°C, (b) 600°C, (c) 700°C, and (d) 800°C.

reason. It should also be noted that the cyclic stability is relatively good after the initial drop. It is not easy to determine which carbon-incorporation method is better for overall performance, because of the mixed results shown in Fig. 6. Nevertheless, it can be said that carbon-incorporation is necessary, for $LiMnBO_3$ to have a meaningful capacity for Li-ion batteries. In addition, the reduced size of $LiMnBO_3$

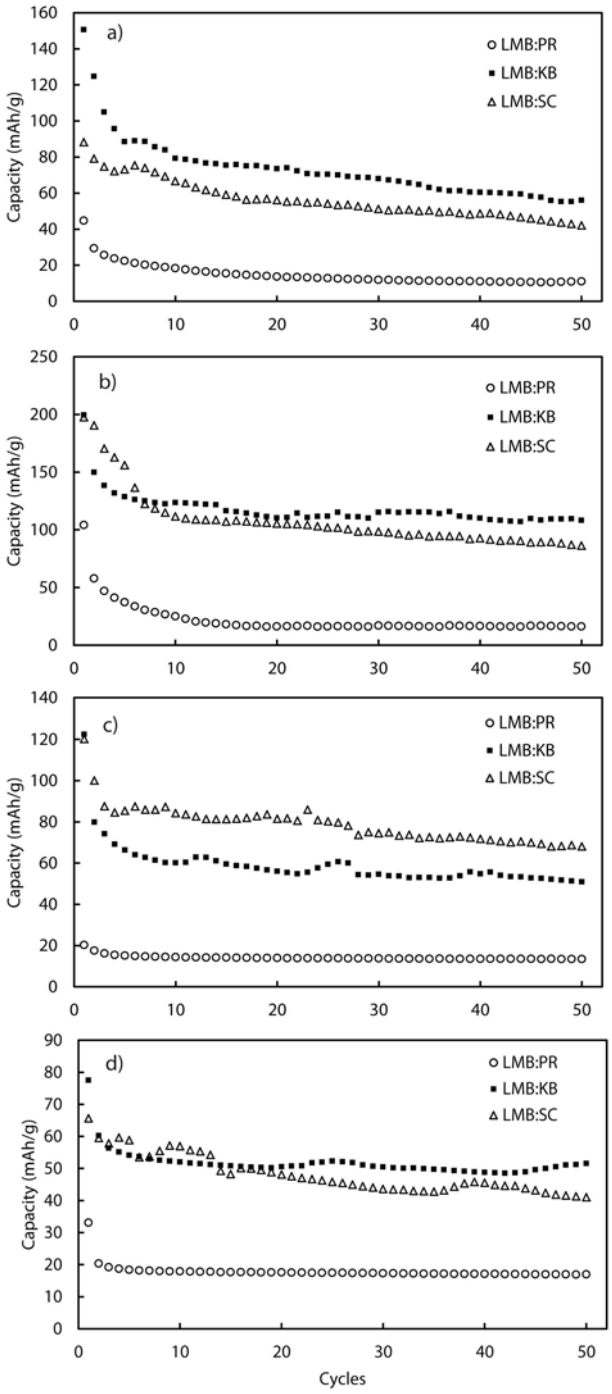

Fig. 6. Charge capacities as a function of cycle number for $LiMnBO_3$ calcined at (a) 500°C, (b) 600°C, (c) 700°C, and (d) 800°C.

via carbon-incorporation should have a favorable effect on the electrochemical performance, as well.

Figure 7 shows the Nyquist plots of differently treated $LiMnBO_3$ calcined at 600°C. The semi-circle at high frequencies corresponds to the charge transfer resistance at the electrode/electrolyte interface, so that the smaller semi-circle of LMB:KB and LMB:SC indicates a lower charge transfer resistance, which should originate from the smaller particle size and enhanced electronic conductivity that results from carbon-incorporation.

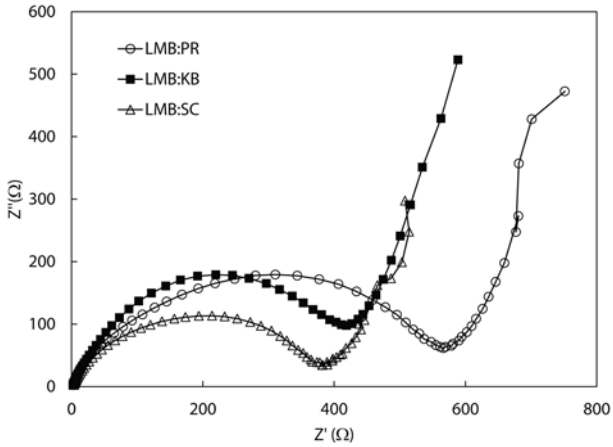

Fig. 7. The Nyquist plots of differently treated $LiMnBO_3$ calcined at 600°C.

4. CONCLUSIONS

Pristine and carbon-incorporated $LiMnBO_3$ is synthesized at various temperatures, and their lithium electrochemical performance is investigated. The $LiMnBO_3$ structure is changed from monoclinic to hexagonal, with an increase of the calcination temperature. Pristine $LiMnBO_3$ shows very limited capacity with large polarization; however, the capacity is hugely increased with carbon-incorporation by ketjen black or sucrose, which not only increases the electronic conductivity, but also suppresses severe particle growth. $LiMnBO_3$ calcined at 600°C, which has mixed phase with 66% monoclinic phase, shows the best electrochemical performance, with the capacity of 108.2 mAh/g after 50 cycles. The most important observation is that the higher capacity can be achieved when $LiMnBO_3$ has monoclinic/hexagonal mixed phase. Based on these results, further improvements can be made, by the reduction of particles size, and the optimization of the mixed phase.

ACKNOWLEDGMENTS

This research was supported by Basic Science Research Program through the National Research Foundation of Korea (NRF) funded by the Ministry of Education, Science and Technology (2012-000860).

REFERENCES

1. J. B. Goodenough and Y. Kim, *Chem. Mater.* **22**, 5872 (2010).
2. T. B. Reddy, *Linden's Handbook of Batteries*, Fourth ed.,

McGraw Hill, New York (2011).
3. A. K. Padhi, K. S. Nanjundaswamy, and J. B. Goodenough, *J. Electrochem. Soc.* **144**, 1188 (1997).
4. H. Song, K. T. Lee, M. G. Kim, L. F. Nazar, and J. Cho, *Adv. Funct. Mater.* **20**, 3818 (2010).
5. R. Mukherjee, R. Krishnan, T.-M. Lu, and N. Koratkar, *Nano Energy* **1**, 518 (2012).
6. B. L. Ellis, K. T. Lee, and L. F. Nazar, *Chem. Mater.* **22**, 691 (2010).
7. Y. Oh, S. Nam, S. Wi, S. Hong, and B. Park, *Electron. Mater. Lett.* **8**, 91 (2012).
8. M.-S. Yoon, M. Islam, Y. M. Park, and S.-C. Ur, *Electron. Mater. Lett*. **9**, 187 (2013).
9. R. Dominko, *J. Power Sources* **184**, 462 (2008).
10. T. Muraliganth, K. R. Stroukoff, and A. Manthiram, *Chem. Mater.* **22**, 5754 (2010).
11. V. Legagneur, Y. An, A. Mosbah, R. Portal, A. Le Gal La Salle, A. Verbaere, D. Guyomard, and Y. Piffard, *Solid State Ionics* **139**, 37 (2001).
12. A. Yamada, N. Iwane, Y. Harada, S. Nishimura, Y. Koyama, and I. Tanaka, *Adv. Mater.* **22**, 3583 (2010).
13. L. Chen, Y. Zhao, X. An, J. Liu, Y. Dong, Y. Chen, and Q. Kuang, *J. Alloy. Compd*. **494**, 415 (2010).
14. Y. Z. Dong, Y. M. Zhao, Z. D. Shi, X. N. An, P. Fua, and L. Chen, *Electrochim. Acta* **53**, 2339 (2008).
15. J. C. Kim, C. J. Moore, B. Kang, G. Hautier, A. Jain, and G. Ceder, *J. Electrochem. Soc.* **158**, A309 (2011).
16. S. Afyon, D. Kundu, F. Krumeich, and R. Nesper, *J. Power Sources* **224**, 145 (2013).
17. O. S. Bondareva, M. A. Simonov, Y. K. Egorovtismenko, and N. V. Belov, *Sov. Phys. Crystallogr*. **23**, 269 (1978).